

Kondo Destruction and Quantum Criticality in Kondo Lattice Systems

Qimiao Si^{1,*}, J. H. Pixley¹, Emilian Nica¹, Seiji J. Yamamoto¹,
Pallab Goswami², Rong Yu³, Stefan Kirchner^{4,5}

¹ *Department of Physics and Astronomy, Rice University, Houston, TX 77005, USA*

² *National High Magnetic Field Laboratory, Florida State University, Tallahassee, FL 32310*

³ *Department of Physics, Renmin University of China, Beijing, 100872, China*

⁴ *Max Planck Institute for the Physics of Complex Systems, 01187 Dresden, Germany*

⁵ *Max Planck Institute for Chemical Physics of Solids, 01187 Dresden, Germany*

Considerable efforts have been made in recent years to theoretically understand quantum phase transitions in Kondo lattice systems. A particular focus is on Kondo destruction, which leads to quantum criticality that goes beyond the Landau framework of order-parameter fluctuations. This unconventional quantum criticality has provided an understanding of the unusual dynamical scaling observed experimentally. It has also predicted a sudden jump of the Fermi surface and an extra (Kondo destruction) energy scale, both of which have been verified by systematic experiments. Considerations of Kondo destruction have in addition yielded a global phase diagram, which has motivated the current interest in heavy fermion materials with variable dimensionality or geometrical frustration. Here we summarize these developments, and discuss some of the ongoing work and open issues. We also consider the implications of these results for superconductivity. Finally, we address the effect of spin-orbit coupling on the global phase diagram, suggest that SmB_6 under pressure may display unconventional superconductivity in the transition regime between a Kondo insulator phase and an antiferromagnetic metal phase, and argue that the interfaces of heavy-fermion heterostructures will provide a fertile setting to explore topological properties of both Kondo insulators and heavy-fermion superconductors.

1. Introduction

Quantum criticality is currently being studied in a wide variety of strongly correlated electron systems. It provides a mechanism for both non-Fermi liquid excitations and unconventional superconductivity. Heavy fermion metals represent a prototype system to study the nature of quantum criticality, as well as the novel phases that emerge in the vicinity of a quantum critical point (QCP).^{1,2}

Over the past decade, Kondo lattice systems have provided a setting for extensive theoretical analysis of quantum phase transitions between ordered antiferromagnetic (AF) and paramagnetic ground states. Various studies have revealed a class of unconventional QCPs that goes beyond the Landau framework of order-parameter fluctuations. This local quantum criticality incorporates the physics of Kondo destruction. Considerations of unconventional quantum criticality have naturally led to the question of the role of Kondo destruction in the emergent phases. Consequently, a global phase diagram has recently been proposed.

In this article, we give a perspective on this subject and discuss the recent developments. We also point out several outstanding issues and some new avenues for future studies.

2. Quantum criticality

A quantum many-body Hamiltonian may contain terms that lead to competing ground states. A textbook example^{3,4} is the problem of a chain of Ising spins, containing both a nearest-neighbor ferromagnetic exchange interaction between the spins and a magnetic field applied along a transverse direction. The exchange interaction favors a ground state in which all the spins are aligned, which spontaneously breaks a global Z_2 symmetry and yields the familiar ferromagnetic order. The

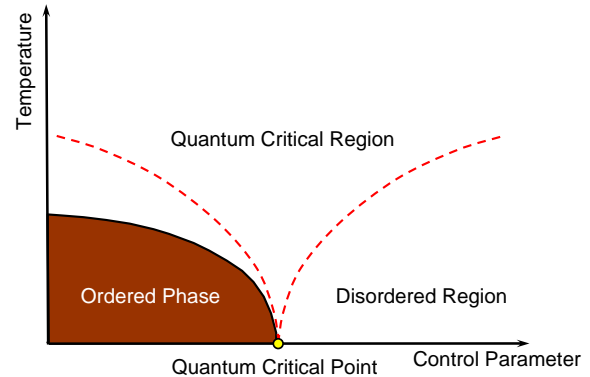


Fig. 1. (Color online) Quantum critical behavior in the generic phase diagram of temperature and a non-thermal control parameter.

transverse field, on the other hand, prefers a ground state in which all the spins point along transverse direction; this state does not spontaneously break any symmetry of the Hamiltonian, and is therefore a magnetically-disordered state.

In general, the ratio of such competing interactions specifies a control parameter, which tunes the system from one ground state to another through a quantum phase transition. A typical case is illustrated in Fig. 1, where the quantum phase transition goes from an ordered state to a disordered one. When it is continuous, the transition occurs at a QCP.

In the Landau framework, the phases are distinguished by an order parameter, which characterizes the spontaneous symmetry breaking. The quantum criticality is then described in terms of $d + z$ -dimensional fluctuations of the order parameter in space and time. Here, d is the spatial dimension and z is the dynamic exponent.

For weak metallic antiferromagnets, the magnetization as

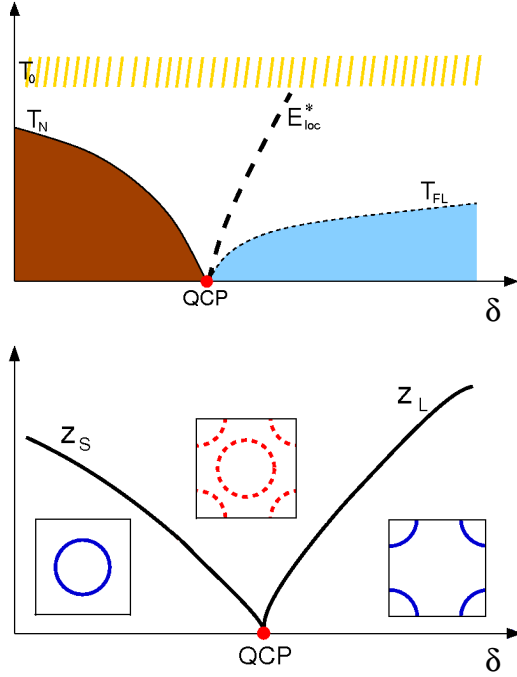


Fig. 2. (Color online) Local quantum criticality (top panel) and the corresponding δ -dependence of the quasiparticle spectral weights z_S and z_L , respectively for small and large Fermi surfaces (bottom panel). Here, $\delta \equiv T_K^0/I$ is the control parameter, and T_0 marks the initial onset of Kondo screening process; T_N and T_{FL} are respectively the Néel and Fermi-liquid temperatures. E_{loc}^* characterizes the Kondo destruction, separating the part of the phase diagram where the system flows towards a Kondo-singlet ground state from that where the flow is towards a Kondo-destroyed ground state. The bottom panel also illustrates the small (left) and large (right) Fermi surfaces, and the fluctuating Fermi surfaces (middle) associated with the QCP.

sociated with the ordering wavevector characterizes a spin-density-wave (SDW) order. The QCP separates the SDW phase from a paramagnetic Fermi liquid state. The collective fluctuations are described in terms of a ϕ^4 theory of order-parameter fluctuations.⁵

In heavy fermion metals, QCPs between an AF phase and a paramagnetic heavy-fermion state have been observed in a number of compounds.^{1,2} The local quantum criticality has new critical modes associated with the destruction of the Kondo effect, in addition to the fluctuations of the AF order parameter.^{6,7} It has provided an understanding of unusual dynamical scaling properties observed in quantum critical heavy fermion metals,^{8,9} and made predictions regarding the evolution of Fermi surfaces and emergence of new energy scales that have been verified by subsequent experiments in YbRh₂Si₂ and CeRhIn₅.^{10–13}

3. From the Kondo Effect to its Destruction

3.1 Kondo effect

The Kondo effect was originally studied in the context of a single-impurity Kondo model:

$$H_{\text{Kondo}} = H_0 + J_K \mathbf{S} \cdot \mathbf{s}_0^c \quad (1)$$

Here, $H_0 = \sum_{\mathbf{k}, \sigma} \varepsilon_{\mathbf{k}} c_{\mathbf{k}\sigma}^\dagger c_{\mathbf{k}\sigma}$, $\mathbf{s}_0^c = c_{0\sigma}^\dagger (\boldsymbol{\tau}_{\sigma\sigma'} / 2) c_{0\sigma'}$, with $\boldsymbol{\tau}$ denoting a vector of Pauli matrices, and $c_{0\sigma}^\dagger$ creates an electron of spin σ at the impurity site 0; the Kondo coupling J_K is antiferromagnetic ($J_K > 0$). The renormalization-group

(RG) beta-function is, to quadratic order:¹⁴

$$\frac{dJ_K}{dl} \equiv \beta(J_K) = J_K^2 \quad (2)$$

The positive sign implies that the effective Kondo coupling grows as the energy is lowered. The RG flow is towards a strong-coupling fixed point, which controls the physics below a bare Kondo energy scale: $T_K^0 \approx \rho_0^{-1} \exp(-1/\rho_0 J_K)$, where ρ_0 is the density of states of the conduction electrons at the Fermi energy. At the strong-coupling fixed point, the local moment and the spins of the conduction electrons are locked into an entangled singlet state:

$$|\text{Kondo singlet}\rangle = \frac{1}{2} (|\uparrow\rangle_f |\downarrow\rangle_{c,FS} - |\downarrow\rangle_f |\uparrow\rangle_{c,FS}) \quad (3)$$

where $|\sigma\rangle_{c,FS}$ represents a linear combination of the conduction-electron states close to the Fermi energy.

This singlet ground state supports a resonance in the low-energy excitation spectrum. The Kondo resonance corresponds to a low-energy electronic excitation, which can clearly be seen in an analysis of the strong-coupling limit, when J_K is taken to be larger than the bandwidth of the conduction electrons, and has been readily described in terms of a slave boson method.¹⁴ The Kondo coupling is converted into an effective hybridization, b^* , between an emergent fermion f_σ and the conduction electrons.

3.2 Kondo lattice and heavy Fermi liquid

In stoichiometric heavy fermion compounds containing, e.g., Ce or Yb elements, the partially-filled $4f$ electrons are strongly correlated. They behave as a lattice of effective spin-1/2 local moments, which describe the magnetic degrees of freedom of the lowest Kramers-doublet atomic levels. This yields a Kondo lattice Hamiltonian:

$$H_{\text{KL}} = H_0 + \sum_{ij} I_{ij} \mathbf{S}_i \cdot \mathbf{S}_j + \sum_i J_K \mathbf{S}_i \cdot \mathbf{s}_i^c \quad (4)$$

The Kondo coupling J_K is antiferromagnetic and we will focus on an antiferromagnetic RKKY interaction, $I_{ij} > 0$.

At high energies, the local moments are essentially decoupled, and Eq. (2) would continue to apply, signifying the initial development of Kondo screening process. What happens in the ground state, however, will depend on the competition between the Kondo and RKKY interactions.

Consider first the regime where the Kondo effect dominates, with T_K^0 being much larger than the RKKY interaction. The physics of this regime can be inferred by taking the bare Kondo coupling J_K to be greater than the bandwidth W of conduction electrons.^{15–17} The Fermi surface will be large, enclosing $1 + x$ electrons per unit cell. When J_K/W is reduced to being considerably smaller than 1, while keeping I/T_K^0 small, continuity dictates that the entangled Kondo singlet state still characterize the ground state, and the Fermi surface will remain large. This can be seen, microscopically, through the slave-boson approach.^{18–20} The Kondo resonance in the excitation spectrum appears as a pole in the conduction-electron self-energy:

$$\Sigma(\mathbf{k}, \omega) = \frac{(b^*)^2}{\omega - \varepsilon_f^*} \quad (5)$$

where the self energy is defined through the Dyson equation:

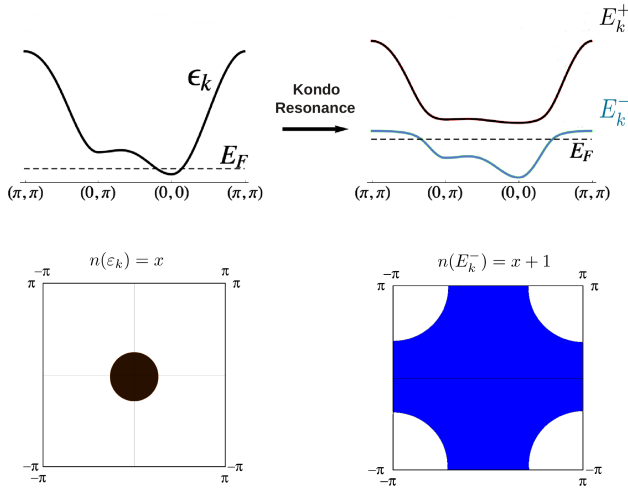


Fig. 3. (Color online) (Left) The energy dispersion of the conduction-electron band. The Fermi surface is small in that it only involves the x conduction electrons per unit cell. (Right) The bands of the hybridized heavy Fermi liquid. A Kondo/hybridization gap separates the two bands. The Fermi surface is large in that it also counts the local moments. Without a loss of generality, we have taken $0 < x < 1$.

$G_c(\mathbf{k}, \omega) = [\omega - \epsilon_{\mathbf{k}} - \Sigma(\mathbf{k}, \omega)]^{-1}$. The conduction-electron Green's function now has two poles, at energies

$$E_{\mathbf{k}}^{\pm} = (1/2)[\epsilon_{\mathbf{k}} + \epsilon_f^* \pm \sqrt{(\epsilon_{\mathbf{k}} - \epsilon_f^*)^2 + 4(b^*)^2}] \quad (6)$$

which describe the heavy-fermion bands. As illustrated in Fig. 3, the nonzero b^* describing the Kondo resonances is directly responsible for a large Fermi surface. The quasiparticle residue goes as $z_L \propto (b^*)^2$ (Fig. 2).

In addition to the Kondo coupling between the local moments and conduction electrons, the Kondo-lattice Hamiltonian also contains an RKKY interaction among the local moments. In Eq. (4), this has been explicitly incorporated. The RKKY interaction I represents an energy scale that competes against T_K^0 , the Kondo scale.^{21,22} We define the ratio of the two energy scales, $\delta \equiv T_K^0/I$, to be the tuning parameter.

Historically, the beginning of the heavy-fermion field focused attention on the Fermi liquid behavior highlighted by a large carrier mass, as well as the exploration of unconventional superconductivity. It was gradually realized that the Fermi liquid description can break down.^{23,24} In the modern era, there is a wide recognition that quantum criticality underlies the non-Fermi liquid behavior in many, if not all, heavy-fermion systems.

3.3 Quantum Criticality: From Landau approach to Kondo destruction

To study quantum criticality in heavy-fermion metals, one would normally assume that the Kondo effect remains intact across the QCP. The ordered state is then a SDW and the QCP follows the Landau approach introduced by Hertz for weak antiferromagnets.^{5,25,26} Because the dynamic exponent in this approach is $z = 2$, the effective dimension $d+z$ is larger than or equal to 4 (the upper critical dimension of the ϕ^4 theory). Therefore, the fixed point is Gaussian.

The search for beyond-Landau quantum criticality has focused on the phenomenon of Kondo destruction, from which

emerges the inherently quantum modes that do not connect with any spontaneous broken symmetry.

To study the Kondo destruction, it is important to analyze the dynamical competition between the RKKY and Kondo interactions. The RKKY interaction induces dynamical correlations among the local moments, which are detrimental to the formation of the Kondo singlets. The important question is whether this effect is sufficiently strong to destroy the amplitude of the static singlet, b^* , and correspondingly drive the energy scale (E_{loc}^*) or temperature scale ($T_{\text{loc}}^* = E_{\text{loc}}^*/k_B$, where k_B is the Boltzmann constant) to zero. Such Kondo destruction was discussed early on in RG analyses of models containing Kondo-lattice-type effects.²⁷⁻³⁰ A systematic study became available in Refs. ^{6,31} which provided an understanding of the anomalous spin dynamics measured⁸ in the quantum critical heavy fermion metal $\text{CeCu}_{5.9}\text{Au}_{0.1}$. These studies also predicted the collapse of the Kondo-destruction energy scale E_{loc}^* , a sudden jump of the Fermi surface across the QCP, and the critical nature of the quasiparticles on the whole Fermi surface at the QCP (cf. Fig. 2). This approach was connected to some general theoretical considerations.⁷ The Kondo destruction has since also been studied in a fermionic slave-particle approach^{32,33} as well as in dynamical mean field theory.³⁴ The critical quasiparticles on the entire Fermi surface have also been considered using a self-consistent method.³⁵

4. Kondo destruction and Quantum Criticality of Antiferromagnetic Heavy Fermion Metals

An AF QCP is expected when the control parameter δ becomes sufficiently small, *i.e.*, when the RKKY interaction is large enough. One microscopic approach that has been playing an important role is the extended dynamical mean-field theory (EDMFT).^{27,36,37}

4.1 EDMFT approach

In the EDMFT approach, the fate of the Kondo effect is studied through the Bose-Fermi Kondo model,

$$\mathcal{H}_{\text{imp}} = H_{\text{Kondo}} + \sum_p w_p \Phi_p^\dagger \cdot \Phi_p + g \sum_p \mathbf{S} \cdot (\Phi_p + \Phi_{-p}^\dagger), \quad (7)$$

along with the self-consistency equations $\chi_{\text{loc}}(\omega) = \sum_{\mathbf{q}} \chi(\mathbf{q}, \omega)$, and $G_{\text{loc}}(\omega) = \sum_{\mathbf{k}} G(\mathbf{k}, \omega)$. Associated with Eq. (7) are the Dyson equations: $M(\omega) = \chi_0^{-1}(\omega) + 1/\chi_{\text{loc}}(\omega)$ and $\Sigma(\omega) = G_0^{-1}(\omega) - 1/G_{\text{loc}}(\omega)$, where $\chi_0^{-1}(\omega) = -g^2 \sum_p 2w_p/(\omega^2 - w_p^2)$ and $G_0(\omega) = \sum_p 1/(\omega - E_p)$. The self-consistency equations manifests spatial dimensionality of the magnetic fluctuations through the form of the RKKY density of states $\rho_I(x) \equiv \sum_{\mathbf{q}} \delta(x - I_{\mathbf{q}})$. Two dimensional magnetic fluctuations correspond to a $\rho_I(x)$ which is nonzero at the lower edge, as typified by the case: $\rho_I(x) = (1/2I)\Theta(I - |x|)$, where Θ is the Heaviside step function. On the other hand, three dimensional magnetic fluctuations are represented by a $\rho_I(x)$ with a square-root form near the lower edge, as given by the example of $\rho_I(x) = (2/\pi I^2)\sqrt{I^2 - x^2}\Theta(I - |x|)$.

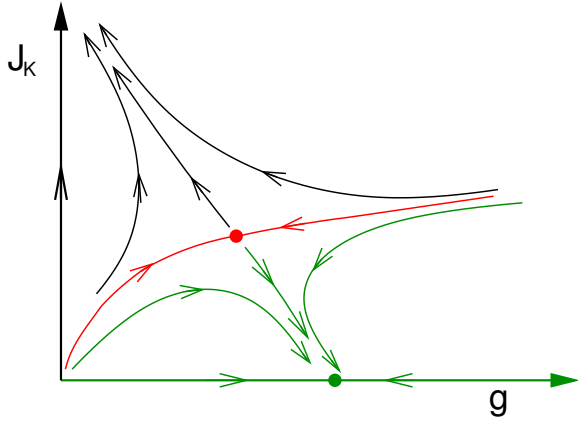


Fig. 4. (Color online) RG flow of the Bose-Fermi Kondo model (with $\epsilon > 0$), showing the strong-coupling Kondo fixed point and its destruction.

4.2 Kondo destruction

In the EDMFT approach, the dynamical magnetic correlations of the local moments influences the Kondo effect through the bosonic bath. Irrespective of the spatial dimensionality, the bosonic bath has a softened spectrum near the magnetic QCP. Correspondingly, it causes an enhanced suppression the Kondo effect. This effect has been studied extensively, as in Ref..³⁸ It can be most clearly seen through an RG approach of the Bose-Fermi Kondo problem that utilizes an ϵ -expansion, where ϵ is defined through the deviation of the bosonic spectrum from the Ohmic form: $\sum_p \delta(\omega - w_p) \sim \omega^{1-\epsilon}$. The RG equations of the Kondo problem, Eq. (2), now have, to the quadratic order in J_K and g^2 , the following form:^{6,28–30,39}

$$\begin{aligned} \beta(J_K) &= J_K(J_K - g^2) \\ \beta(g) &= g(\epsilon/2 - g^2) \end{aligned} \quad (8)$$

The RG equations yield a Kondo-destruction critical point, as shown in Fig. 4. Importantly, the zero-temperature local spin susceptibility has the form:

$$\chi_{\text{loc}}(\tau) \sim \tau^{-\epsilon} \quad (9)$$

Importantly, the result for the critical exponent is valid to infinite orders in ϵ .

4.3 Local quantum critical point

The EDMFT equations have been studied in some detail in a number of analytical and numerical studies.^{6,31,40–44} Irrespective of the spatial dimensionality, the weakening of the Kondo effect is seen through the reduction of the E_{loc}^* scale as we approach the QCP from the paramagnetic side.

E_{loc}^* vanishes at the QCP for two-dimensional magnetic fluctuations. The dynamical spin susceptibility satisfies the following dynamical scaling:

$$\chi(\mathbf{q}, \omega) = \frac{1}{f(\mathbf{q}) + A(-i\omega)^\alpha \mathcal{M}(\omega/T)} \quad (10)$$

The exponent α is found to be near to 0.75 (between 0.72 and 0.83 derived from different approaches).^{40,43,44}

For three-dimensional magnetic fluctuations, E_{loc}^* is reduced but remains non-zero at the QCP. It however terminates inside the ordered portion of the phase diagram (see below).

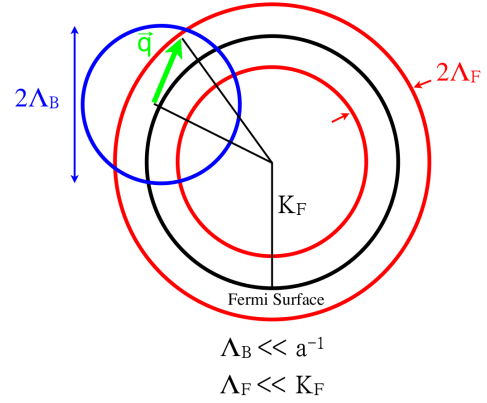


Fig. 5. (Color online) Different kinematics in the scaling of the bosonic and fermionic sectors. Figure adapted from Ref..⁵⁵

In both cases, the zero-temperature transition is second-order when the effective RKKY interaction appears in the same form on both sides of the transition.^{45,46} It is important to stress one effect that is crucial for both the stability of the Kondo-destroyed AF phase as well as the second-order nature of the QCP: a dynamical Kondo effect still operates in the Kondo-destroyed AF phase. We will expound on this point in Sec. 6.

5. Global phase diagram

Kondo destruction and the associated Fermi-surface change represent physics that goes beyond the Landau framework. Considerations of new phases that reflect this physics have led to a global phase diagram for the AF Kondo-lattice systems.^{47–49} This phase diagram was first developed based on theoretical studies showing the stability of the AF_S phase.^{47,50–52} This is an AF phase with Kondo destruction and an associated small Fermi surface.

5.1 Kondo destruction inside antiferromagnetic order: QNL σ M approach

Can the Kondo effect be destroyed inside the AF ordered phase? To address this issue, Ref.⁵⁰ considered the model with SU(2) symmetry, and in the parameter limit of $J_K \ll I \ll W$. (The case with Ising anisotropy is simpler: because the AF-ordered phase has a spin gap, J_K is irrelevant and the AF_S phase will be stable.) We consider the reference limit $J_K = 0$ to be the local moments in a collinear AF order, described by a quantum non-linear sigma model (QNL σ M) and, separately, the conduction electron band. The QNL σ M^{53,54} takes the form:

$$\mathcal{S}_{\text{QNL}\sigma\text{M}} = (c/2g) \int d^d x d\tau \left[(\nabla \mathbf{n})^2 + c^{-2} (\partial_\tau \mathbf{n})^2 \right], \quad (11)$$

where c is the spin-wave velocity and g measures the amount of quantum fluctuations, which grows as the amount of frustration is increased (such as via tuning the ratio of next nearest neighbor to nearest neighbor spin-spin interactions on a square lattice).

The case of the AF zone boundary not intersecting the Fermi surface of the conduction electrons allows an asymptotically exact analysis. Expressed in terms of the \mathbf{n} field of the QNL σ M, which represents the staggered magnetization,

the Kondo coupling takes the following form at low energies:

$$\mathcal{S}_K = \lambda_K \int d^d x d\tau \mathbf{s}_c \cdot \mathbf{n} \times \partial_\tau \mathbf{n}. \quad (12)$$

While the RG procedure⁵⁵ appropriate for combined gapless fermionic⁵⁶ and bosonic fields is in general very involved, the situation simplifies here because the QNL σ M has a dynamic exponent $z = 1$. The kinematics involved in the RG approach is illustrated in Fig. 5. The resulting RG equation is:

$$\beta(\lambda_K) = 0 \quad (13)$$

In other words, λ_K is exactly marginal. The Kondo coupling does not grow, and there is no Kondo singlet formation in the ground state; *i.e.*, the AF phase has a Kondo destruction. This establishes the stability of the AF_S phase. A large- N analysis of the low-energy excitations was also carried out in Ref.,⁵⁰ yielding a self-energy for the conduction electrons:

$$\Sigma(\mathbf{k}, \omega) \propto \omega^d. \quad (14)$$

This self-energy lacks a pole, which is to be contrasted with Eq. (5). In other words, the Kondo resonance is absent, and the Fermi surface is small.

5.2 Global Phase Diagram

The stability of the AF_S phase raises the question, what are the different possible routes to suppress AF order and tune the system from the AF_S phase towards the paramagnetic heavy-fermion state (P_L phase)? The routes are illustrated in the global phase diagram, Figure 6. This zero-temperature phase diagram involves two parameters: in addition to the Kondo coupling J_K , there is also G which measures the degree of the quantum fluctuations of the local-moment magnetism. The vertical axis reflects tuning geometrical frustration or dimensionality. The Kondo coupling, depicted as the horizontal axis, is taken to be dimensionless with the conduction-electron bandwidth W as the normalization factor. The global phase diagram itself is a two-dimensional projection of a multi-dimensional phase diagram. In particular, we have considered the case with a fixed I/W that is considerably smaller than 1. In addition, we have fixed, x , the number of conduction electrons per site, to some non-integer value.

There are three sequences of phase transitions from the AF_S phase to the P_L phase. Trajectory I represents a direct transition involving Kondo destruction, and corresponds to the local QCP. Trajectory II involves an intermediate AF_L phase, which represents the SDW order of the P_L phase. There is a Kondo-destruction transition inside the AF order, while the AF to non-magnetic transition is of the SDW type. Trajectory III involves an intermediate P_S phase, which could involve non-magnetic order such as a valence-bond solid.

5.3 Specific cases and multiplicity of tuning parameters

Our discussion so far is very general. To make further progress, it is important to consider the specific cases as well as the specific realizations of the parameter G .

One case which is amenable to concrete calculations is the Ising-anisotropic Kondo problem in the presence of a transverse magnetic field. As already mentioned in the introduction, the transverse field introduces quantum fluctuations of the local-moment magnetism, which is captured by the G parameter.

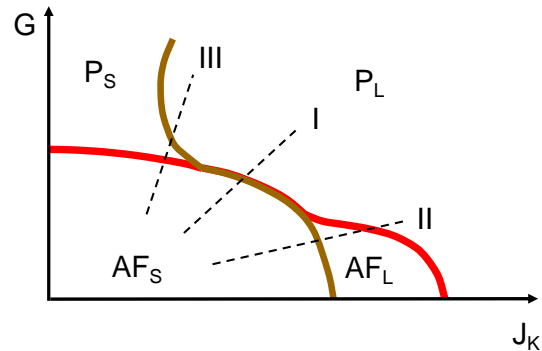


Fig. 6. The global phase diagram of the AF Kondo lattice.^{47,48} This $T = 0$ phase diagram involves a frustration axis (G) and an axis that tunes the Kondo coupling (J_K). P_L and P_S are paramagnetic phases whose Fermi surfaces are respectively large and small (*i.e.* with or without Kondo resonances). AF_L and AF_S are their AF counterparts.

In an EDMFT study, this leads to a Bose-Fermi Kondo model, with Ising anisotropy and in the presence of a transverse field, which is supplemented by self-consistency conditions. The transverse-field Bose-Fermi Kondo model *per se* has recently been studied in detail.⁵⁷ The calculations have been carried out using a version of the numerical renormalization group method,⁵⁸ and a line of Kondo-destruction fixed points was identified.

Another setting for concrete calculations is the spin-symmetric Kondo lattice model on the Shastry-Sutherland lattice. The parameter J_2/J_1 – the ratio of the exchange interaction on a diagonal bond to that on the nearest-neighbor bond – measures the degree of frustration and is defined as G . A key advantage is that, at large G and $J_K = 0$ the ground state of the local-moment only model is known exactly to be a valence-bond solid.⁵⁹ A large- N -based calculation⁶⁰ yields a phase diagram that is reminiscent of Fig. 6 when the conduction electrons are away from half-filling.

5.4 Berry phase and the topological defects of Néel order

Considerations of the global phase diagram also opens up the study of the heavy-fermion state based on the Berry phase and topological defects of local-moment magnetism. This was recently studied in the QNL σ M representation of the spin one-half Kondo lattice model on a honeycomb lattice at half filling,⁶¹ (see also Ref. ⁶² for the 1D case). It has been shown that the skyrmion defects of the antiferromagnetic order parameter host a number of competing states. In addition to the spin Peierls, charge and current density wave order parameters, Kondo singlets also appear as the competing variables dual to the AF order. In this basis, the conduction electrons acquire a Berry phase through their coupling to the hedgehog configurations of the Néel order, which cancels the Berry phase of the local moments. These results demonstrate the competition between the Kondo-singlet formation and spin-Peierls order when the AF order is suppressed, in a way that is compatible with the global phase diagram discussed earlier.

6. Antiferromagnetic order: Kondo destruction vs. spin-density-wave order

We have so far emphasized that the stability of the AF_S phase has been derived based on an (asymptotically exact) RG

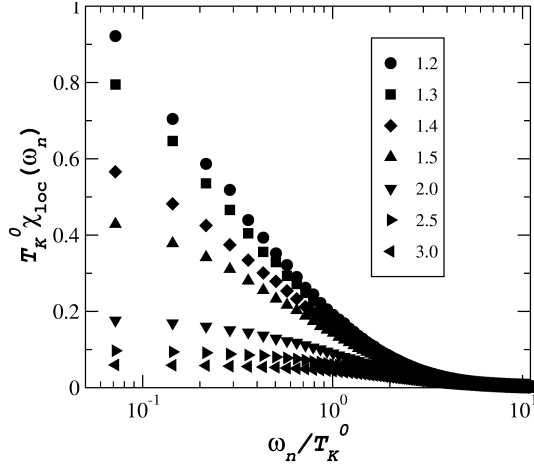


Fig. 7. Dynamical Kondo effect in the AF_S phase, for various values of I/T_K^0 on the ordered side.⁶³

analysis. The exact marginality of the Kondo coupling inside the AF order is to be contrasted with its marginal relevance in the paramagnetic case. Because the effective Kondo coupling does not grow, the system no longer flows to the strong-coupling Kondo fixed point; in the ground state, the static Kondo singlet has zero amplitude. However, the marginal nature of the effective Kondo coupling also implies that the Kondo coupling influences the properties at non-zero energies. In other words, a dynamical Kondo effect operates.

This analysis complements the results from the EDMFT studies in the ordered state. Figure 7 shows the local dynamical spin susceptibility as a function of frequency in the AF_S state.⁶³ Its increase as δ is tuned towards the QCP reflects the growth of the dynamical Kondo effect. When δ reaches δ_c , the local dynamics in the ordered state match the quantum critical behavior determined from the EDMFT studies in the absence of the order. This demonstrates the importance of the dynamical Kondo effect in ensuring the second-order nature of the zero-temperature transition. The same conclusions also emerge in several other studies.^{43,44}

Indeed, the dynamical Kondo effect is important for the stability of the AF_S phase. It allows the gain of the Kondo exchange energy even in the absence of the static Kondo singlet formation. This point is important to understand the results of several variational Quantum Monte Carlo studies.^{64–66} These studies used a variational wavefunction for the AF_S phase that not only sets the static Kondo amplitude to zero, but also disallows any Kondo fluctuations at finite energies. As such, it cannot energetically compete against the AF_L phase, defined in terms of a variational wavefunction with a static Kondo-singlet amplitude. In this way, the approach does not adequately capture the dynamical competition between the RKKY and Kondo interactions. Correspondingly, it is difficult to stabilize the AF_S phase. Instead, these studies would only allow the multiple AF ground states with a Lifshitz transition inside the SDW AF_L phase. In the example shown in Fig. 8, this corresponds to going from the usual AF_L phase for small AF order parameter, with co-existing electron and hole pockets, to the AF_{L2} phase for larger AF order parameter, in which the hole pocket has disappeared. Interestingly, the standard DMFT approach likewise over-emphasizes the

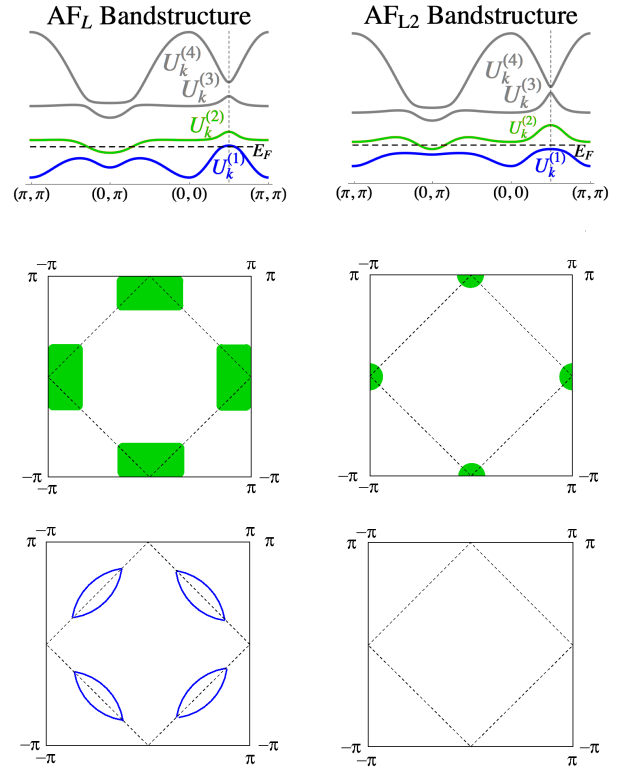


Fig. 8. (Color online) AF_L and AF_{L2} phases in the SDW portion of the phase diagram. U_k^α , with $\alpha = 1, \dots, 4$, are the heavy-fermion bands in the presence of a staggered field associated with a staggered magnetization.

Kondo coupling, because the RKKY interactions do not appear in the dynamical equations [the bosonic bath in Eq. (7) is absent in DMFT]. The approach therefore reduces the regime of stability of the AF_S phase.⁶⁷ In the terminology of Fig. 6, it captures the type II transition but misses the type I transition (or, for that matter, the type III transition as well).

7. Experiments on quantum critical heavy fermions

Quantum phase transitions in general, and Kondo destruction in particular, have been playing a central role in the modern studies of heavy fermion magnetism and superconductivity. Here we briefly consider the salient properties of the theory that have either been compared to known experiments, or represent predictions that have been tested by subsequent experiments. More extensive discussions may be found in Refs..^{68,69}

We have already mentioned the strong evidence^{8,10–13} for local quantum criticality from the heavy-fermion compounds $CeCu_{6-x}Au_x$, $YbRh_2Si_2$, and $CeRhIn_5$. This concerns the anomalous dynamical scaling, an extra energy scale and a sudden jump of the Fermi surface. Additional evidence has come from transport measurements^{70–72} in $CeRhIn_5$ and NMR studies of $YbRh_2Si_2$.⁷³

The proposed global phase diagram has helped understand a surprisingly rich zero-temperature phase diagram of the Ir- and Co-substituted $YbRh_2Si_2$.^{74,75} Likewise, it may also provide a means to understand the variety of quantum phase transitions under the multiple tuning parameters in $CeCu_{6-x}Au_x$ ⁷⁶ and $CeRhIn_5$.⁷⁷

The global phase diagram has suggested that increasing dimensionality tunes the occurrence of Kondo destruction from

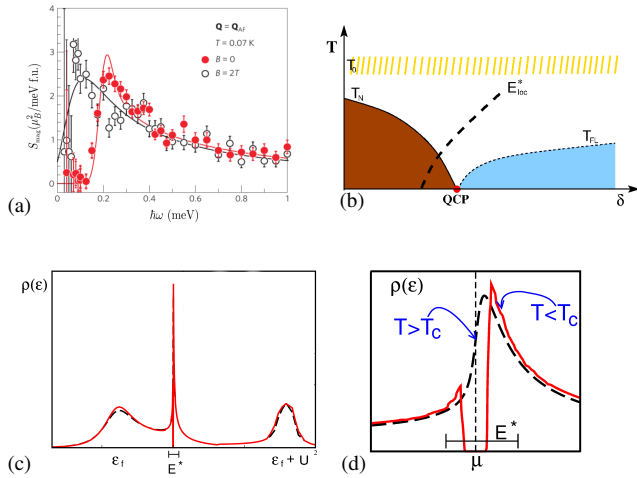


Fig. 9. (Color online) (a) Dynamical spin structure factor in the normal and superconducting states of CeCu_2Si_2 , from Ref.⁸³ (b)(c)(d) Interpretation of the large exchange energy gain in terms of a nonzero but small Kondo-destruction energy scale E_{loc}^* , as introduced in Refs.^{83,84} and described in the main text.

at the onset of AF order to inside the ordered region, which is consistent with the measurements in $\text{Ce}_3\text{Pd}_{20}\text{Si}_6$.⁷⁸

Finally, it also suggests that heavy-fermion materials with lattices that host geometrically-frustrated magnetism would be particularly instructive in exploring the upper portion of the phase diagram, *i.e.* the region where the local-moment component contains especially strong quantum fluctuations. This has provided the motivation for recent studies of heavy-fermion metals on Shastry-Sutherland,⁷⁹ Kagome,⁸⁰ fcc⁸¹ and triangular⁸² lattices.

8. Implications for superconductivity

Unconventional superconductivity often arises in the vicinity of magnetic instabilities.⁸⁵ At the same time, the superconducting phases found in rare earth intermetallic compounds have rich and diverse properties. It is therefore natural to suspect that the global phase diagram for the heavy fermions with its various magnetic transitions will have implications for the emergence of superconductivity. That antiferromagnetic spin fluctuations promote unconventional superconductivity has been suggested^{86,87} soon after the discovery of unconventional superconductivity in CeCu_2Si_2 by F. Steglich.⁸⁸ Inelastic neutron scattering spectroscopy of the normal and superconducting state of CeCu_2Si_2 near quantum criticality showed that the gain in exchange energy across the transition is an order of magnitude larger than the condensation energy.⁸³ (Related conclusion has also been reached in CeCoIn_5 .⁸⁹) While establishing that the magnetism drives the formation of superconductivity, it also implies that a correspondingly large kinetic energy is lost across the superconducting transition. This has been interpreted in terms of a Kondo-destruction energy scale E_{loc}^* being nonzero but quite small: this allows the further reduction of the Kondo-singlet amplitude by superconductivity to transfer substantial amount of Kondo-resonance spectral weight to higher energies, causing a large loss of the Kondo screening energy which is counted as a part of the kinetic energy. Indeed, there has been considerable evidence by now that the low-energy and low-

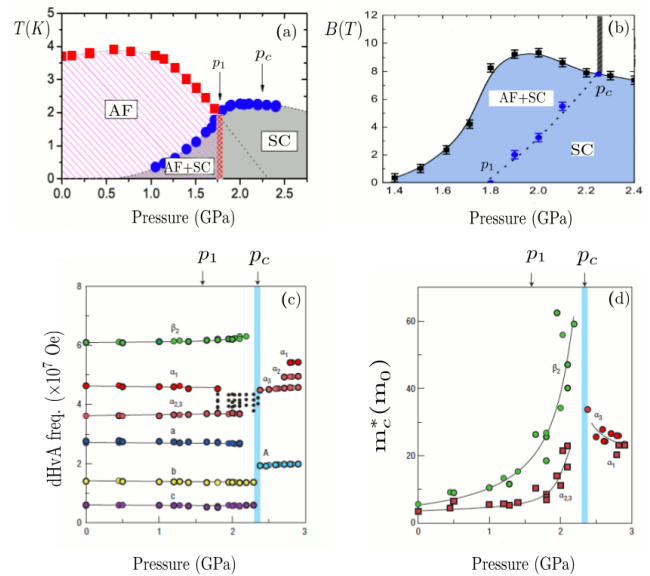


Fig. 10. (Color online) Phase diagram of CeRhIn_5 in the T - p plane at zero field (a) and in the B - p plane close to zero temperature (b); figures adapted from Ref..⁷⁰ Also shown is the dHvA measurements as a function of pressure, showing a sudden jump of dHvA frequencies (c), which indicates a corresponding jump of the Fermi surface, and a tendency of divergence in the effective mass (d); figures adapted from Ref..¹¹

QCP,^{90,91} but the dynamics above a relatively low temperature (~ 1 K) appears to be consistent with the non-SDW, ω/T , scaling form;⁹¹ this suggests that E_{loc}^* at the QCP is on the order of 1 K. In recent years, STM studies have been carried out in a number of heavy-fermion systems.^{92,93} We anticipate that the kinetic energy loss can be estimated through STM measurements of the single-particle spectral function both in the normal and superconducting states.

The evidence for the Kondo destruction quantum criticality determining superconductivity is the most direct in CeRhIn_5 (Refs.^{11,70}). In this compound under pressure, AF order is weakened and eventually gives way to superconductivity,⁹⁴ as shown in Fig. 10(a); $T_c \approx 2.3$ K is high in that it is about 10% of the bare Kondo temperature. Applying a magnetic field suppresses superconductivity and uncovers an AF QCP, as seen in Fig. 10(b). Across this QCP, the Fermi surface experiences a sudden jump [Fig. 10(c)]. This provides evidence for Kondo destruction, which is corroborated by the divergence of the effective mass [Fig. 10(d)]. All these suggest that the high-temperature superconductivity in CeRhIn_5 originates from local quantum criticality.⁷⁰

9. Spin-orbit coupling and topological phases

9.1 Global phase diagram of Kondo insulators

A generalization to the commensurate conduction-electron filling of $x = 1$ leads to the corresponding global phase diagram for Kondo insulators,⁵² shown in Fig. 11. As discussed elsewhere,⁶⁸ various material families could be considered as candidates for inducing transitions between these different phases.

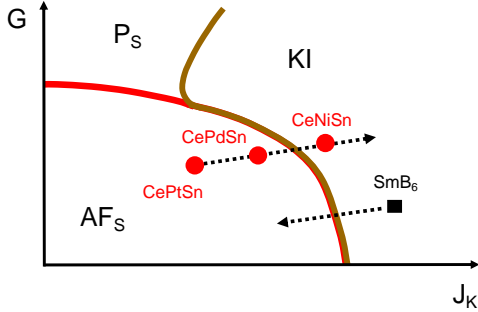


Fig. 11. (Color online) Global phase diagram of Kondo insulators,⁵² and representative materials that may be tuned through various transitions.⁶⁸ Figure adapted from Ref..⁶⁸

9.2 Topological phases and their transitions to magnetic and Kondo states

SmB_6 has been the focus of many renewed experiments.^{95,96} These have followed the suggestion that the strong spin-orbit coupling of the 4f-electrons induce non-trivial topology in the heavy-fermion bandstructure, which turn the Kondo insulator into a topological insulator (TI).⁹⁷ At the present time, there is considerable evidence for surface states in SmB_6 , and whether these are the boundary states of the bulk TI phase remains to be established. Still, it is instructive to consider SmB_6 as a case in which the bulk KI gap can be closed by the application of pressure. When that happens, the system becomes metallic and magnetically ordered,⁹⁸ making the trajectory of phase transition to be likely along the dashed line shown in Fig. 11.

With this in mind, it is intriguing to note the transport evidence for non-Fermi liquid behavior in SmB_6 under a pressure of about 4 GPa, in the transition regime.⁹⁹ This suggests that the zero-temperature transition from the KI phase to the AF_S is (close to being) second order, and the associated QCP underlies the non-Fermi liquid behavior. Given the stoichiometric nature of the system, it would then be natural to suggest that superconductivity will appear in a similar pressure range as a consequence of quantum criticality.

Another transition at a Kondo-insulator filling is between a P_S phase and a KI phase.¹⁰⁰ This has been studied in a Kondo lattice model supplemented by a spin-orbit coupling (SOC) for the conduction electrons:

$$H = H_{KL} + H_{soc}(c) \quad (15)$$

The details of the Hamiltonian are given in Ref..¹⁰⁰ The spin-orbit coupling term in this Hamiltonian induces a topological insulator state for the conduction electrons. Because of the TI gap of the conduction electrons, the Kondo coupling J_K must be larger than a non-zero threshold value J_K^c in order to reach a Kondo insulator phase. A large-N analysis yields a continuous transition between the TI and Kondo insulator phases. It is likely that magnetic order will also interplay with these phases, and studying this effect in the model should be very instructive.

9.3 Heavy fermion interfaces

Such consideration of the spin-orbit coupling also suggests the intriguing possibility of new properties at the interface of

heavy-fermion heterostructures. Because of the broken inversion symmetry at the interface, the heavy electrons in the interface layer should contain an extra SOC of the Rashba type: $\mathcal{H}_{soc} = \sum_{\mathbf{k}} V_{soc}(\mathbf{n} \times \mathbf{k}) \cdot \mathbf{s}(\mathbf{k})$, where \mathbf{k} is the wavevector, V_{soc} the spin-orbit coupling, \mathbf{n} the unit vector perpendicular to the interface, and $\mathbf{s}(\mathbf{k})$ the spin of the electrons with wavevector \mathbf{k} . For the oxide heterostructures, a Rashba-type SOC with V_{soc} on the order of 5 meV has been demonstrated.^{101,102} Such a SOC energy scale will be competitive against the heavy-fermion energy scales, raising the possibility for topologically non-trivial superconducting or insulating states at such heavy-fermion interfaces. Heavy-fermion heterostructures appear to be quite realistic to study. For instance, heavy-fermion superlattices have recently been fabricated and studied.^{103,104}

10. Summary and Outlook

With the ever expanding family of heavy fermion materials suitable for studying quantum criticality, there is no doubt that new insights will continue to be gained from these systems on general issues of non-Fermi liquid behavior and unconventional superconductivity. Here, we have focused our attention on an important theme, namely how Kondo destruction influences quantum criticality and the formation of novel phases.

We have emphasized that quantum criticality that results from Kondo destruction in Kondo lattice system goes beyond the standard spin-density-wave type. More generally, we have considered how the physics of Kondo destruction leads to a global magnetic phase diagram. The latter has motivated recent theoretical studies on the interplay between magnetic frustration and Kondo screening, as well as the experimental exploration of heavy-fermion compounds with varied dimensionality or geometrical frustration.

We have also provided evidence that superconductivity in some of the canonical heavy-fermion systems is influenced, or even dominated, by the Kondo-destruction physics of the normal state. Developing a framework to study superconductivity in such an unconventional quantum critical setting is a pressing theoretical issue.

Finally, we have discussed how spin-orbit coupling introduces new type of transitions between topological states and magnetic or Kondo coherent phases. Pressurizing SmB_6 appears to induce such a transition; the tantalizing evidence for the (nearly) second-order nature of this transition leads us to suggest that SmB_6 under a pressure of about 4 GPa might superconduct as a result of the collapsing of the Kondo-insulator gap and the simultaneous development of antiferromagnetic order. For related reasons, we have argued that the interface of heavy-fermion heterostructures could be a fertile ground to study the interplay between topological electronic structure, magnetism and superconductivity.

We would like to thank J. Dai, L. Deng, X.-Y. Feng, K. Ingersent, J. Wu, J.-X. Zhu and L. Zhu for collaborations on the various theoretical aspects covered here, E. Abrahams, M. Brando, S. Friedemann, C. Geibel, P. Gegenwart, C. Krellner, S. Paschen, H. Pfau, F. Steglich, and S. Wirth for collaborations on the quantum criticality in YbRh_2Si_2 , and S. Paschen for collaborations on the phase diagram of $\text{Ce}_3\text{Pd}_{20}\text{Si}_6$ as well as instructive discussions on Kondo insulators. This work has been supported in part by the NSF Grant No. DMR-1309531 and the Robert A. Welch Foundation Grant No. G-14111. DC

acknowledges the support of the NSF Cooperative Agreement No.DMR- 0654118, the State of Florida and the U. S. Department of Energy.

- 1) Special issue: Quantum Phase Transitions. *J. Low Temp. Phys.* **161**, 1-323 (2010).
- 2) Q. Si and F. Steglich: *Science* **329** (2010) 1161.
- 3) P. Pfeuty: *Ann. Phys. (N.Y.)* **57** (1970) 79.
- 4) A. P. Young: *J. Phys. C* **8** (1975) L309.
- 5) J. Hertz: *Phys. Rev. B* **14** (1976) 1165.
- 6) Q. Si, S. Rabello, K. Ingersent, and J. Smith: *Nature* **413** (2001) 804.
- 7) P. Coleman, C. Pépin, Q. Si, and R. Ramazashvili: *J. Phys. Cond. Matt.* **13** (2001) R723.
- 8) A. Schröder, G. Aeppli, R. Coldea, M. Adams, O. Stockert, H. v. Löhneysen, E. Bucher, R. Ramazashvili, and P. Coleman: *Nature* **407** (2000) 351.
- 9) M. Aronson, R. Osborn, R. Robinson, J. Lynn, R. Chau, C. Seaman, and M. Maple: *Phys. Rev. Lett.* **75** (1995) 725.
- 10) S. Paschen, T. Lühmann, S. Wirth, P. Gegenwart, O. Trovarelli, C. Geibel, F. Steglich, P. Coleman, and Q. Si: *Nature* **432** (2004) 881.
- 11) H. Shishido, R. Settai, H. Harima, and Y. Onuki: *J. Phys. Soc. Jpn.* **74** (2005) 1103.
- 12) P. Gegenwart, T. Westerkamp, C. Krellner, Y. Tokiwa, S. Paschen, C. Geibel, F. Steglich, E. Abrahams, and Q. Si: *Science* **315** (2007) 969.
- 13) S. Friedemann, N. Oeschler, S. Wirth, C. Krellner, C. Geibel, F. Steglich, S. Paschen, S. Kirchner, and Q. Si: *PNAS* **107** (2010) 14547.
- 14) A. C. Hewson: *The Kondo Problem to Heavy Fermions* (Cambridge University Press, Cambridge, 1997).
- 15) Q. Si, arXiv:1012.5440, a chapter in book edited by L. D. Carr: *Understanding Quantum Phase Transitions*, 2010.
- 16) Lacroix, C.: *Solid State Commun.* **54** (1985) 991.
- 17) P. Nozières: *Eur. Phys. J. B* **6** (1998) 447.
- 18) A. Auerbach and K. Levin: *Phys. Rev. Lett.* **35** (1987) 3394.
- 19) A. J. Millis and P. A. Lee: *Phys. Rev. B* (1987).
- 20) S. Burdin, A. Georges, and D. R. Grempel: *Phys. Rev. Lett.* **85** (2000) 1048.
- 21) S. Doniach: *Physica B* **91** (1977) 231.
- 22) C. M. Varma: *Rev. Mod. Phys.* **48** (1976) 219.
- 23) M. B. Maple, C. L. Seaman, D. A. Gajewski, Y. Dalichaouch, V. B. Barbetta, M. C. de Andrade, H. A. Mook, H. G. Lukefahr, O. O. Bernal, and D. E. MacLaughlin: *J. Low Temp. Phys.* **95** (1994) 225.
- 24) G. R. Stewart: *Rev. Mod. Phys.* **73** (2001) 797.
- 25) A. J. Millis: *Phys. Rev. B* **48** (1993) 7183.
- 26) T. Moriya: *Spin Fluctuations in Itinerant Electron Magnetism* (Springer, Berlin, 1985).
- 27) Q. Si and J. L. Smith: *Phys. Rev. Lett.* **77** (1996) 3391.
- 28) J. L. Smith and Q. Si: arXiv:cond-mat/9705140, *Europhys. Lett.* **45** (1999) 228.
- 29) A. M. Sengupta: arXiv:cond-mat/9707316, *Phys. Rev. B* **61** (2000) 4041.
- 30) Q. Si, J. L. Smith, and K. Ingersent: *Int. J. Mod. Phys. B* **13** (1999) 2331.
- 31) Q. Si, S. Rabello, K. Ingersent, and J. Smith: *Phys. Rev. B* **68** (2003) 115103.
- 32) T. Senthil, M. Vojta, and S. Sachdev: *Phys. Rev. B* **69** (2004) 035111.
- 33) I. Paul, C. Pépin, and M. R. Norman: *Phys. Rev. Lett.* **98** (2007) 026402.
- 34) L. D. Leo, M. Civelli, and G. Kotliar: *Phys. Rev. Lett.* **101** (2008) 256404.
- 35) P. Wölfle and E. Abrahams: *Phys. Rev. B* **84** (2011) 041101(R).
- 36) J. L. Smith and Q. Si: *Phys. Rev. B* **61** (2000) 5184.
- 37) R. Chitra and G. Kotliar: *Phys. Rev. Lett.* **84** (2000) 3678.
- 38) L. Zhu, S. Kirchner, Q. Si, and A. Georges: *Phys. Rev. Lett.* **93** (2004) 267201.
- 39) L. Zhu and Q. Si: *Phys. Rev. B* **66** (2002) 024426.
- 40) D. Grempel and Q. Si: *Phys. Rev. Lett.* **91** (2003) 026401.
- 41) J. Zhu, D. Grempel, and Q. Si: *Phys. Rev. Lett.* **91** (2003) 156404.
- 42) P. Sun and G. Kotliar: *Phys. Rev. Lett.* **91** (2003) 027200.
- 43) M. Glossop and K. Ingersent: *Phys. Rev. Lett.* **99** (2007) 227203.
- 44) J.-X. Zhu, S. Kirchner, R. Bulla, and Q. Si: *Phys. Rev. Lett.* **99** (2007) 227204.
- 45) Q. Si, J.-X. Zhu, and D. R. Grempel: *J. Phys.: Condens. Matter* **17** (2005) R1025.
- 46) P. Sun and G. Kotliar: *Phys. Rev. B* **71** (2005) 245104.
- 47) Q. Si: *Physica B* **378** (2006) 23.
- 48) Q. Si: *Phys. Status Solidi B* **247** (2010) 476.
- 49) P. Coleman and A. Nevidomskyy: *J. Low Temp. Phys.* **161** (2010) 182.
- 50) S. J. Yamamoto and Q. Si: *Phys. Rev. Lett.* **99** (2007) 016401.
- 51) T. T. Ong and B. A. Jones: *Phys. Rev. Lett.* **103** (2009) 066405.
- 52) S. J. Yamamoto and Q. Si: *J. Low Temp. Phys.* **161** (2010) 233.
- 53) F. D. M. Haldane: *Phys. Rev. Lett.* **50** (1983) 1153.
- 54) S. Chakravarty, B. I. Halperin, and D. R. Nelson: *Phys. Rev. B* **39** (1989) 2344.
- 55) S. Yamamoto and Q. Si: *Phys. Rev. B* **81** (2010) 205106.
- 56) R. Shankar: *Rev. Mod. Phys.* **66** (1994) 129.
- 57) E. M. Nica, K. Ingersent, J.-X. Zhu, and Q. Si: *Phys. Rev. B* **88** (2013) 014414.
- 58) M. T. Glossop and K. Ingersent: *Phys. Rev. Lett.* **95** (2005) 067202.
- 59) B. S. Shastry and B. Sutherland: *Physica B* **108** (1981) 1069.
- 60) J. H. Pixley, R. Yu, and Q. Si: arXiv:1309.0581 (2013).
- 61) P. Goswami and Q. Si: arXiv:1309.0501 (2013).
- 62) P. Goswami and Q. Si: *Phys. Rev. Lett.* **107** (2011) 126404.
- 63) J. Zhu, D. Grempel, and Q. Si: *Phys. Rev. Lett.* **91** (2003) 156404.
- 64) H. Watanabe and M. Ogata: *Phys. Rev. Lett.* **99** (2007) 136401.
- 65) L. C. Martin and F. F. Assaad: *Phys. Rev. Lett.* **101** (2008) 066404.
- 66) N. Lanatà, P. Barone, and M. Fabrizio: *Phys. Rev. B* **78** (2008) 155127.
- 67) S. Hoshino and Y. Kuramoto: *Phys. Rev. Lett.* **111** (2013) 026401.
- 68) Q. Si and S. Paschen: *Phys. Status Solidi B* **250** (2013) 425.
- 69) F. Steglich, et. al.: arXiv:1309.7260 (2013).
- 70) T. Park, F. Ronning, H. Q. Yuan, M. B. Salamon, R. Movshovich, J. L. Sarrao, and J. D. Thompson: *Nature* **440** (2006) 65.
- 71) T. Park, V. A. Sidorov, F. Ronning, J.-X. Zhu, Y. Tokiwa, H. Lee, E. D. Bauer, R. Movshovich, J. L. Sarrao, and J. D. Thompson: *Nature* **456** (2008) 366.
- 72) G. Knebel, D. Aoki, J.-P. Brison, and J. Flouquet: *J. Phys. Soc. Jpn.* **77** (2008) 114704.
- 73) K. Ishida, K. Okamoto, Y. Kawasaki, Y. Kitaoka, O. Trovarelli, C. Geibel, and F. Steglich: *Phys. Rev. Lett.* **89** (2002) 107202.
- 74) S. Friedemann, T. Westerkamp, M. Brando, N. Oeschler, S. Wirth, P. Gegenwart, C. Krellner, C. Geibel, and F. Steglich: *Nature Phys.* **5** (2009) 465.
- 75) J. Custers, P. Gegenwart, C. Geibel, F. Steglich, P. Coleman, and S. Paschen: *Phys. Rev. Lett.* **104** (2010) 186402.
- 76) O. Stockert, M. Enderle, and H. v. Löhneysen: *Phys. Rev. Lett.* **99** (2007) 237203.
- 77) L. Jiao, et. al.: arXiv:1308.0294 (2013).
- 78) J. Custers, K. Lorenzer, M. Müller, A. Prokofiev, A. Sidorenko, H. Winkler, A. M. Strydom, Y. Shimura, T. Sakakibara, R. Yu, Q. Si, and S. Paschen: *Nature Mater.* **11** (2012) 189.
- 79) M. S. Kim and M. C. Aronson: *Phys. Rev. Lett.* **110** (2013) 017201.
- 80) V. Fritsch, N. Bagrets, G. Goll, W. Kitzler, M. J. Wolf, K. Grube, C.-L. Huang, and H. v. Löhneysen: arXiv:1301.6062 (2013).
- 81) E. D. Mun, S. L. Bud'ko, C. Martin, H. Kim, M. A. Tanatar, J.-H. Park, T. Murphy, G. M. Schmiedeshoff, N. Dilley, R. Prozorov, and P. C. Canfield: *Phys. Rev. B* **87** (2013) 075120.
- 82) D. D. Khalyavin, D. T. Adroja, P. Manuel, A. Daoud-Aladine, M. Kosaka, K. Kondo, K. A. McEwen, J. H. Pixley, and Q. Si: *Phys. Rev. B* **87** (2013) 220406.
- 83) O. Stockert, J. Arndt, E. Faulhaber, C. Geibel, H. S. Jeevan, S. Kirchner, M. Loewenhaupt, K. Schmalzl, W. Schmidt, Q. Si, and F. Steglich: *Nat. Phys.* **7** (2011) 119.
- 84) O. Stockert, S. Kirchner, F. Steglich, and Q. Si: *J. Phys. Soc. Jpn.* **81** (2012) 011001.
- 85) N. Mathur, F. Grosche, S. Julian, I. Walker, D. Freye, R. Haselwimmer, and G. Lonzarich: *Nature* **394** (1998) 39.
- 86) D. J. Scalapino, E. Loh, and J. E. Hirsch: *Phys. Rev. B* **34** (1986) 8190.
- 87) K. Miyake, S. Schmitt-Rink, and C. M. Varma: *Phys. Rev. B* **34** (1986) 6554.
- 88) F. Steglich, J. Aarts, C. Bredl, W. Lieke, D. Meschede, W. Franz, and H. Schäfer: *Phys. Rev. Lett.* **43** (1979) 1892.

- Rev. Lett. **100** (2008) 087001.
- 90) P. Gegenwart, C. Langhammer, C. Geibel, R. Helfrich, M. Lang, G. Sparn, F. Steglich, R. Horn, L. Donnevert, A. Link, and W. Assmus: Phys. Rev. Lett. **81** (1998) 1501.
- 91) J. Arndt, O. Stockert, K. Schmalzl, E. Faulhaber, H. S. Jeevan, C. Geibel, W. Schmidt, M. Loewenhaupt, and F. Steglich: Phys. Rev. Lett. **106** (2011) 246401.
- 92) A. R. Schmidt, M. H. Hamidian, P. Wahl, F. Meier, A. V. Balatsky, J. D. Garrett, T. J. Williams, G. M. Luke, and J. C. Davis: Nature **465** (2010) 570.
- 93) P. Aynajian, E. H. da Silva Neto, A. Gyenis, R. E. Baumbach, J. D. Thompson, Z. Fisk, E. D. Bauer, and A. Yazdani: Nature **486** (2012) 201.
- 94) H. Hegger, C. Petrovic, E. G. Moshopoulou, M. F. Hundley, J. L. Sarrao, Z. Fisk, and J. D. Thompson: Phys. Rev. Lett. **84** (2000) 4986.
- 95) S. Wolgast, C. Kurdak, K. Sun, J. W. Allen, D.-J. Kim, and Z. Fisk: (arXiv:1211.5104) (2012).
- 96) J. Botimer, D. J. Kim, S. Thomas, T. Grant, Z. Fisk, and J. Xia: (arXiv:1211.6769) (2012).
- 97) M. Dzero, K. Sun, V. Galitski, and P. Coleman: Phys. Rev. Lett. **104** (2010) 106408.
- 98) A. Barla, J. Derr, J. P. Sanchez, B. Salce, G. Lapertot, B. P. Doyle, R. Ruffer, R. Lengsdorf, M. M. Abd-Elmeguid, and J. Flouquet: Phys. Rev. Lett. **94** (2005) 166401.
- 99) S. Gabáni, E. Bauer, S. Berger, K. Flachbart, Y. Paderno, C. Paul, V. Pavlík, and N. Shitsevalova: Phys. Rev. B **67** (2003) 172406.
- 100) X.-Y. Feng, J. Dai, C.-H. Chung, and Q. Si: (arXiv:1206.0979), Phys. Rev. Lett. **111** (2013) 016402.
- 101) A. D. Caviglia, M. Gabay, S. Gariglio, N. Reyren, C. Cancellieri, and J.-M. Triscone: Phys. Rev. Lett. **104** (2010) 126803.
- 102) M. Ben Shalom, M. Sachs, D. Rakhmievitch, A. Palevski, and Y. Dagan: Phys. Rev. Lett. **104** (2010) 126802.
- 103) H. Shishido, T. Shibauchi, K. Yasu, T. Kato, H. Kontani, T. Terashima, and Y. Matsuda: Science **327** (2010) 980.
- 104) S. K. Goh, Y. Mizukami, H. Shishido, D. Watanabe, S. Yasumoto, M. Shimozawa, M. Yamashita, T. Terashima, Y. Yanase, T. Shibauchi, A. I. Buzdin, and Y. Matsuda: Phys. Rev. Lett. **109** (2012) 157006.